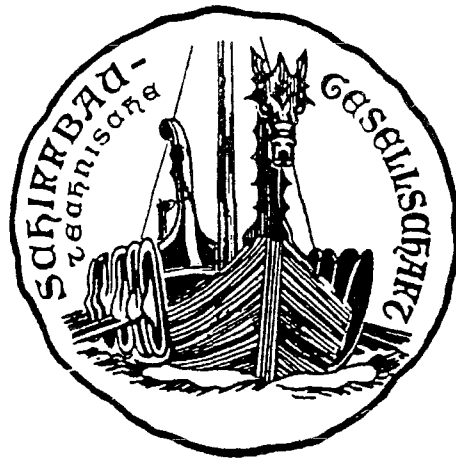


STG - Nr. 3007

**Schiffbautechnische Gesellschaft e. V.
Hamburgische Schiffbau-Versuchsanstalt GmbH**



International Symposium
on
Propulsors and Cavitation

22 - 25 June, 1992
Hamburg, Germany

Harmonic Cascading in Bubble Clouds

S. Kumar, Palaiseau, France
C. E. Brennen, Pasadena, CA, USA

ABSTRACT

Nonlinear interactive effects in a bubbly cloud have been studied by investigating the frequency response of a bubble layer bounded by a wall oscillating normal to itself. First, a Fourier analysis of the Rayleigh-Plesset equation is used to obtain an approximate solution for the nonlinear response of a single bubble in an infinite fluid. This is used to solve for nonlinear effects in a semi-infinite layer containing bubbles with a distribution of size.

A phenomena termed *harmonic cascading* is seen to take place due to presence of distribution of bubble sizes. This phenomena consists of a large response at twice the excitation frequency when the mixture contains bubbles with a natural frequency equal to twice the excitation frequency. The ratio of the amplitude of the second harmonic response to the amplitude of the first harmonic response is observed to increase when the number of small bubbles is increased relative to the number of large bubbles. The response is also seen to be weakened by an increase in the total number of bubbles per unit liquid volume at constant void fraction.

1. INTRODUCTION

The purpose of this research is to gain some understanding of the global effects of bubble dynamics in the fluid mechanics of bubbly flows and, in particular, cavitating flows. At the most basic level, bubble-bubble interactions occur because the pressure changes generate rapid bubble volume changes which cause accelerating velocity fields which effect the pressure distribution in the flow. These effects may occur in the kinds of bubbly cavitating flow which produce noise, damage, and performance deterioration in ship propellers, hydrofoils and turbomachines. The understanding of flows of bubbly mixtures is also important in the design and operation of sonar systems, cavitation detection devices and in acoustical techniques of flow measurement.

Traditionally, cavitating flows have been studied using single bubble dynamics and assuming no interaction among the bubbles in the flow field. Such an approach ignores the interactive effects that the bubble dynamics have on the global pressure distribution in the flow field and is accurate only in case of extremely dilute bubble concentrations. The experimental results of Arakeri and Shanmuganathan (1985) and Marboe *et al.* (1986) have shown that noise pro-

duced by travelling bubble cavitation can be modified by interactive effects at higher bubble concentrations in ways that can not be explained on the basis of single bubble theories. To model these effects researchers have used continuum models incorporating bubble dynamics to analyze global interactive effects. Early studies treated the bubbly mixture as an equivalent compressible homogeneous medium (Tangren, Dodge and Seifert (1949)). Among the first to focus on the dynamics of bubble clusters was van Wijngaarden (1964) who analyzed the collapse of a large number of bubbles next to a flat wall and found considerable increase in the pressure at the wall as result of the interactive effects. Biesheuvel and van Wijngaarden (1984) used ensemble and volume averaging of the conservation equations for each phase to develop more general equivalent flow models of dispersed two phase mixtures, including the phenomena of bubble dynamics, relative motion and liquid compressibility. Most of the later research efforts are based on these equations. d'Agostino and Brennen (1988) and Omta (1987) found that the characteristic natural frequencies of a spherical cloud of bubbles can be much smaller than the natural frequency of a single bubble. Chahine (1982) pioneered other approach to solution the flow of bubble clouds which utilises the method of matching asymptotic expansions and sums up the contribution of individual bubbles in the cloud. Birnir and Smereka (1990) have carried out numerical solutions for bubble clouds and investigated the solutions using techniques used to study dynamical systems. They found that the bubble radius, the flow velocity and pressure were bounded and the cloud was seen to possess natural frequencies.

However, most of the recent analyses use linearized models of the bubble dynamics and the flow. It is well known that the dynamics of a bubble can be quite nonlinear (Prosperetti (1975)) which in combination with nonlinear convective effects may produce significant nonlinear effects in bubbly flows. An attempt to understand these nonlinear effects by studying an analytically amenable model problem is presented here. The purpose is to obtain a qualitative understanding of the various mechanisms of frequency dispersion in the bubbly two phase mixtures associated with cavitation. The dynamics of a bubbly liquid next to a flat wall which oscillates normal to its own plane has been studied. Almost all of the work reported in the literature assume the clouds to contain

identical bubbles. A semi-infinite layer with a given *bubble size distribution* has been examined and reveals new phenomena of *harmonic cascading* in such clouds.

2. NOMENCLATURE

i	imaginary number
k	polytropic constant for gas expansion and contraction
j, m, n	integer indices
l_r	reference length scale
p	pressure in liquid flow field
P_{g0}	pressure of permanent gas in the bubble at undisturbed condition
P_n	complex amplitude of pressure oscillation at frequency $n\delta$
P_o	reference pressure in the liquid
P_v	vapor pressure inside the bubble
P_∞	pressure at infinity
R	radius of the bubble
R_m	radius of the smallest bubbles in the layer
R_M	radius of the largest bubbles in the layer
R_o	radius of the bubble at undisturbed reference conditions
R_n	complex amplitude of radius oscillation at frequency $n\delta$
S	surface tension of the liquid
t	time
T	Lagrangian time
u	velocity of the liquid
x	Eulerian space coordinate normal to the wall
X	Lagrangian space coordinate normal to the wall
X_n	complex amplitude of fluid displacement oscillation at frequency $n\delta$
α	volume fraction of bubbly mixture
α_o	volume fraction of bubbly mixture at undisturbed reference conditions
δ	increment in the frequency
γ	ratio of specific heats
ν	kinematic viscosity
ω_b	natural frequency of the bubble (in radians/sec)
ω_f	forcing frequency for pressure or wall oscillation (in radians/sec)
ω_r	reference frequency (in radians/sec)
$\eta(R_o)$	bubble number density per unit liquid volume
$\eta^*(R_o)$	bubble number density per unit total volume
η'	number of bubbles per unit liquid volume
\Re	real part of complex quantity
ρ	density of the liquid
ρ_v	density of the vapor in the bubble
τ	volume of the bubble
τ_n	complex amplitude of the bubble volume oscillation at frequency $n\delta$
τ_o	volume of the bubble at undisturbed reference conditions

3. SOME TYPICAL APPLICATIONS AND VALUES

Clouds of cavitation bubbles occur in a variety of technological situations. Cavitation clouds are generated by propellers and are an important source of noise and damage. Furthermore, single bubbles in travelling bubble cavitation have been observed to breakup into

many smaller bubbles (Blake *et al.* (1977) and Ceccio and Brennen (1991)) and the dynamics of these small clouds are clearly important. The typical data used for illustration of the present analysis have been selected with these physical situations in mind.

A number of researchers have measured the size of free stream nuclei (Gates and Acosta (1978)) and cavitation bubbles (Maeda *et al.* (1991)). Typical nuclei range in size from 10 μm to 150 μm ; the size distribution can usually be approximated by

$$\eta(R_o) = \frac{N^*}{R_o^m} \quad (1)$$

where $\eta(R_o) dR_o$ is the number of nuclei per unit liquid volume with equilibrium radii between R_o and $R_o + dR_o$. A distribution of the form given by the equation (1) has been used to describe the size distribution of free stream nuclei in sea water and various water tunnel facilities with $N \approx 10^{-5}$ and $m \approx 3 \rightarrow 4$ (Brennen and Ceccio (1989)). The bubble size distribution in cavitation clouds (Maeda *et al.* (1991)) can also be approximately described by equation (1) with suitable values of N^* and m .

The void fraction values due to free stream nuclei are extremely small. Though the void fraction for a cavitation cloud is larger than that of free stream, it is still small at approximately 0.03% (Maeda *et al.* (1991)). No measurements of the void fraction of a cloud resulting from the breakup of a collapsing bubble exist. For purpose of illustrating the present results, void fractions were estimated from the experiments of Arakeri and Shanmuganathan (1985). The fluid has been chosen to be water at room temperature (20 ° C). A bubble subject to periodic excitation oscillates with value of the polytropic constant, k , between 1 and γ (Plesset and Hsieh (1960)) and so, for illustrative purposes, the value of the polytropic constant, k , has been chosen to be 1. When a distribution of bubble sizes is used the form given by equation (1) will be employed and a range of nuclei sizes between 10 μm and 100 μm will be used. The values of ambient pressure have been chosen to be typical values for reduced pressure in the water tunnel (13146 Pa) and atmospheric conditions for cavitation at the ocean surface (101325 Pa). These will be referred to as *Water Tunnel* and *Ocean* conditions.

4. NONLINEAR SOLUTION FOR A SINGLE BUBBLE

There exists a substantial body of literature on the nonlinear dynamics of a single bubble in an infinite fluid (Plesset and Prosperetti (1977)). In the present work it is necessary to construct the very simplest nonlinear solution of the Rayleigh-Plesset equation for a single bubble. Later this will be used as a building block for the problems of many bubbles interacting in a flow. The bubble is assumed to be spherical and to contain water vapor and residual permanent gas. The bubble interior is assumed to be uniform with constant vapor pressure, P_v . The permanent gas in the bubble is assumed to behave polytropically with an index, k , between 1 and γ (Plesset and Hsieh (1960)). The liquid compressibility is only included in the radiation damping and this is done by including it in the effective viscosity used for the bubble dynamics (Devin (1959) and Prosperetti (1977)). The bubble growth due to rectified diffusion has been ignored since

that takes place at a much slower time scale than the natural cycle of the bubble (Hsieh and Plesset (1961)). With these assumptions the Rayleigh-Plesset equation describing the bubble dynamics becomes

$$R \frac{D^2 R}{Dt^2} + \frac{3}{2} \left(\frac{DR}{Dt} \right)^2 + \frac{4\nu}{R} \frac{DR}{Dt} + \frac{2S}{\rho R} = \frac{P_v - P_\infty(t)}{\rho} + \frac{P_{go}}{\rho} \left(\frac{R_o}{R} \right)^{3k} \quad (2)$$

In the present solution a Fourier series expansion is used and terms up to second order are retained in order to examine these corrections to the linear solution. The bubble radius, $R(t)$, and the pressure at infinity, $P_\infty(t)$, are expanded in the form

$$R = R_o + \sum_{n=1}^N \Re(R_n e^{in\delta t}) \quad (3)$$

$$\frac{P_\infty(t)}{\rho} = P_o + \sum_{n=1}^N \Re(P_n e^{in\delta t}) \quad (4)$$

where P_n and R_n are complex quantities and the frequencies $n\delta$, $n = 1, N$ represent a discretization of the frequency domain. These expansions are substituted into equation (2) and all terms of third or higher order in R_n/R_o are neglected in order to extract the simplest nonlinear effects. Finally, coefficients of $e^{in\delta t}$ on both sides of the simplified equation are equated to yield the following relation for P_n and R_n :

$$\frac{P_n}{\omega_b^2 R_o^2} = \Lambda(n) \frac{R_n}{R_o} + \sum_{j=1}^{n-1} \beta_1(n, j) \frac{R_j}{R_o} \frac{R_{n-j}}{R_o} + \sum_{j=1}^{N-n} \beta_2(n, j) \frac{\bar{R}_j}{R_o} \frac{R_{n+j}}{R_o} \quad (5)$$

where the overbar denotes complex conjugate and the bubble natural frequency, ω_b is given by

$$\omega_b = \left(\frac{3k P_{go}}{\rho R_o^2} - \frac{2S}{\rho R_o^3} \right)^{\frac{1}{2}} \quad (6)$$

and $\Lambda(n)$, $\beta_1(n, j)$ and $\beta_2(n, j)$ are defined as

$$\Lambda(n) = \left[\frac{n^2 \delta^2}{\omega_b^2} - 1 - i \frac{n\delta}{\omega_b} \frac{4\nu}{\omega_b R_o^2} \right] \quad (7)$$

$$\beta_1(n, j) = \frac{3k+1}{4} + \frac{3k-1}{2} \frac{S}{\rho \omega_b^2 R_o^3} + \frac{1}{2} \frac{\delta^2}{\omega_b^2} (n-j) \left(n + \frac{j}{2} \right) + i \frac{2\nu}{\omega_b R_o^2} \frac{\delta}{\omega_b} (n-j) \quad (8)$$

and

$$\beta_2(n, j) = \frac{3k+1}{2} + (3k-1) \frac{S}{\rho \omega_b^2 R_o^3} + \frac{1}{2} \frac{\delta^2}{\omega_b^2} (n^2 - nj - j^2) + i \frac{2\nu}{\omega_b R_o^2} \frac{n\delta}{\omega_b} \quad (9)$$

Using a Newton-Raphson scheme, equation (5) is solved iteratively for R_n/R_o given P_n , the fluid properties and individual bubble characteristics. It was seen numerically that if there is a single excitation frequency, ω_f , then the only non-zero components of the

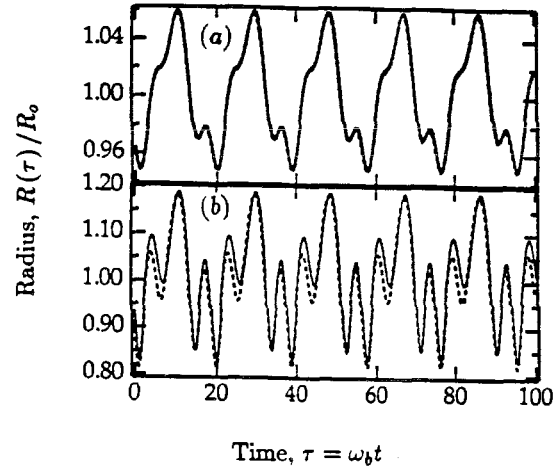


Figure 1. Radius, $R(\tau)/R_o$, is plotted against the nondimensional time, $\tau = \omega_b t$, for a single bubble of 14 μm radius for (a) $P_n/\omega_b^2 R_o^2 = 0.04$ and (b) $P_n/\omega_b^2 R_o^2 = 0.08$. The parameters: $\omega_b/\omega_f = 3.0$ and $\nu/\omega_b R_o^2$ and $S/\rho \omega_b^2 R_o^3$ are for the water tunnel conditions. (—) is the numerical solution and (---) is the approximate analytical solution

bubble oscillation, R_n , will occur at harmonics of that single excitation frequency. It is also seen that the response R_n/R_o decays with increase in the order of the harmonic and is negligible (amplitude $\ll 10^{-20}$) at harmonics of order higher than 50. Thus calculating the response up to 50 harmonics was considered sufficient. It is also clear from the equations (8) and (9) that $\beta_1(n, j)$ and $\beta_2(n, j)$ are functions of $n\delta/\omega_b$ and j/n . Furthermore, note from equation (5) that for a single excitation frequency, the only coefficients $\beta_1(n, j)$ and $\beta_2(n, j)$ which enter the calculations are those for which j and n take values corresponding to harmonics of the excitation frequency. Consequently the only values of $n\delta/\omega_b$ and j/n which enter the calculations are those which are ratios of an excitation frequency harmonic to the natural frequency of the bubble or two excitation frequency harmonics. Hence, despite the explicit appearance of δ , the results of the calculation are independent of this parameter used in discretizing the frequency domain. Finally, note also that the pressure perturbations, P_n , occur in (5) only in linear form and thus can be large without introducing error into the solution. However, the analysis is valid only for $|R_n/R_o| \ll 1$. This defines the extent of the weak nonlinear effects which are examined here and indirectly implies an upper limit on the magnitude of $P_n/\omega_b^2 R_o^2$.

For illustrative purposes, we select the values of the parameters $\nu/\omega_b R_o^2$ ($= 0.01$) and $S/\rho \omega_b^2 R_o^3$ ($= 0.10$) at the water tunnel condition for a bubble of 14 μm radius. We chose to consider a single bubble subjected to an oscillating pressure at infinity containing a single frequency, ω_f , such that $\omega_b/\omega_f = 3.0$ and several values of $P_n/\omega_b^2 R_o^2$. Results obtained from equation (5) are compared to a numerical integration of the Rayleigh-Plesset equation (which uses a fourth order Runge-Kutta scheme) in Fig. 1 for $P_n/\omega_b^2 R_o^2 = 0.04$ and 0.08. It can be seen that present approximate analysis works very well for the smaller amplitude and

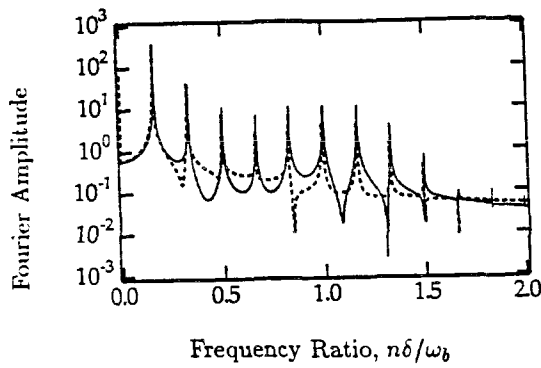


Figure 2. Comparison of the spectra of $[1 - R(t)/R_0]$ obtained for a single bubble of $14 \mu\text{m}$ radius from numerical integration of the Rayleigh-Plesset equation (—) and the present approximate (---) analysis. The parameters: $P_n/\omega_b^2 R_0^2 = 0.08$, $\omega_b/\omega_f = 6.0$ and $\nu/\omega_b R_0^2$ and $S/\rho\omega_b^2 R_0^3$ are for the water tunnel conditions.

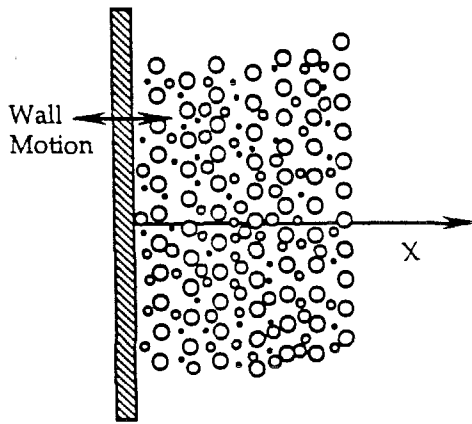


Figure 3. Schematic of the Oscillating Wall Problem.

begins to show some discrepancies at larger amplitude.

It was previously noted that the equation (5) has a nonzero solution only at the harmonics of excitation frequency. However, at present, it is impossible to prove the uniqueness of the solution for nonlinear equations such as the equation (5). The agreement demonstrated in Fig. 1 adds some confidence that the present solutions are unique.

A comparison of the spectra of $[1 - R(t)/R_0]$ is made in Fig. 2 for the case in which the $P_n/\omega_b^2 R_0^2$ and ω_b/ω_f values are 0.08 and 6 respectively. It can be seen that the present approximate solution agrees well with the numerical integration for frequencies at which the magnitude is significant. Note that the radius oscillations occur at harmonics of the frequency of the pressure oscillation, ω_f .

Eller and Flynn (1969) observed that for pressure oscillations with amplitude larger than a threshold value, the bubble radius oscillation will contain a subharmonic of order one half. This can also be seen in Lauterborn (1976)'s numerical calculation of the frequency response of a single bubble and in the 3rd or-

der perturbation solution of Prosperetti (1975). The present solution does not give rise to subharmonics in the domain of its validity, i.e., $|R_n/R_0| \ll 1$. This is because the subharmonics are generated by nonlinearities at an order higher than quadratic. Thus, the absence of subharmonics from our approximate solution does not invalidate our analysis.

More accurate nonlinear solutions than the one described above (for example Prosperetti (1974)) exist and have been reported in the literature. The value of present solution lies in its simplicity and the feasibility of incorporating it in analysis of the collective response of a cloud of bubbles.

5. A SEMI-INFINITE LAYER WITH BUBBLE SIZE DISTRIBUTION

Most of the research efforts in modelling bubbly mixtures so far have assumed bubbly mixtures of identical bubbles. In most practical circumstances, uniformly sized bubbles are very difficult if not impossible to achieve. Moreover, cavitation nuclei in water have a distribution of bubble sizes ranging over several orders of magnitude (Gates and Acosta (1978)).

In this section, we present a weakly nonlinear model of flows of such bubbly mixtures. Since the flow now has a number of length and time scales in terms of the bubble radii and their natural periods, we can expect different mechanisms causing interactions between the different time scales. We shall find a new mechanism for frequency dispersion called *harmonic cascading*.

The specific problem addressed in this analysis is shown schematically in Fig. 3. Liquid containing bubbles is bounded by a flat wall which oscillates in a direction normal to itself at a frequency, ω_f . The resulting flow is assumed to be a function of x and t alone. A number of simplifying assumptions are introduced in order to obtain a soluble set of equations. The volume of liquid involved in condensation and evaporation during bubble oscillation has been ignored; this is reasonable in view of large differences in the density of liquid and vapor phases. The liquid has been assumed to be incompressible and the relative motion between the phases has been ignored. Both were found by d'Agostino and Brennen (1988) to have very little effect on important features such as natural frequencies of the flow. The most important feature of these effects is the damping that they cause at the resonant frequencies. This can be incorporated in the present solution by taking an appropriate value of effective viscosity in place of liquid viscosity used in the Rayleigh-Plesset equation.

We assume that the bubble number density distribution, $\eta(R_0)$, is known and that it is piecewise uniform. Then, the number of bubbles per unit liquid volume with equilibrium size between R_0 and $R_0 + dR_0$ is $\eta(R_0) dR_0$. The volume of bubbles per unit liquid volume is

$$\frac{\alpha}{1 - \alpha} = \int_{R_m}^{R_M} \eta(R_0) \tau dR_0 \quad (10)$$

where τ is the volume of a bubble and R_m and R_M are minimum and maximum equilibrium bubble radii present in the layer. Thus, the number of bubbles per unit total volume with equilibrium radius between R_0

and $R_o + dR_o$, can be written as

$$\eta^*(R_o) dR_o = \eta(R_o)(1 - \alpha) dR_o = \frac{\eta(R_o) dR_o}{1 + \int_{R_m}^{R_M} \eta(R_o) \tau dR_o} \quad (11)$$

We use a dispersed phase number continuity equation to ensure mass and number conservation. Assuming the liquid to be incompressible, it follows that if the bubbles are neither created nor destroyed then

$$\frac{D}{Dt} \int_{R_m}^{R_M} \eta^*(R_o) dR_o + \frac{\partial u}{\partial x} \int_{R_m}^{R_M} \eta^*(R_o) dR_o = 0 \quad (12)$$

Assuming that the number density per unit total volume is conserved, the above equation reduces to

$$\frac{D\eta^*(R_o)}{Dt} + \eta^*(R_o) \frac{\partial u}{\partial x} = 0 \quad (13)$$

The corresponding momentum equation is

$$\rho(1 - \alpha) \frac{Du}{Dt} = -\frac{\partial p}{\partial x} \quad (14)$$

The solution to the problem represented by (2), (11) (13) and (14) was solved in Lagrangian coordinates, X and T using a method parallel to that described in Kumar(1991). The above equations ((13) and (14)) become

$$\frac{\partial \eta^*(R_o)}{\partial T} \frac{\partial x}{\partial X} + \eta^*(R_o) \frac{\partial u}{\partial X} = 0 \quad (15)$$

and

$$\rho \frac{\partial u}{\partial T} \frac{\partial x}{\partial X} = -\frac{1}{1 - \alpha} \frac{\partial P}{\partial X} \quad (16)$$

Consistent with the structure of the solution sought, the relationship between Lagrangian and Eulerian coordinates, X and x , is written in the form

$$x = X + \sum_{n=1}^N \Re(X_n(X) e^{in\delta T}) \quad (17)$$

and the bubble volume, τ , and pressure, P , are written as

$$\tau = \tau_o + \sum_{n=1}^N \Re(\tau_n(X) e^{in\delta T}) \quad (18)$$

$$\frac{P}{\rho} = P_o + \sum_{n=1}^N \Re(P_n(X) e^{in\delta T}) \quad (19)$$

Substituting the expansion (18) into equation (10) we obtain

$$\int_{R_m}^{R_M} \eta(R_o) \tau dR_o = \frac{\alpha_o}{1 - \alpha_o} + \sum_{n=1}^N \Re(A_n e^{in\delta T}) \quad (20)$$

where

$$A_n = \int_{R_m}^{R_M} \eta(R_o) \tau_n dR_o \quad (21)$$

The above equations ((15), (16) and (20)) along with the expansions ((17), (18) and (19)) have been used to yield following governing equation for the pressure oscillations in the layer (Kumar (1991))

$$\frac{d^2 (P_n / \omega_r^2 l_r^2)}{d(X/l_r)^2} = \lambda_n^2 \frac{P_n}{\omega_r^2 l_r^2} + \sum_{j=1}^{n-1} \psi(n, j) \frac{P_j}{\omega_r^2 l_r^2} \frac{P_{n-j}}{\omega_r^2 l_r^2} + \sum_{j=1}^{N-n} \theta(n, j) \frac{\bar{P}_j}{\omega_r^2 l_r^2} \frac{P_{n+j}}{\omega_r^2 l_r^2} \quad (22)$$

where

$$\lambda_n^2 = (1 - \alpha_o)^2 \left(\frac{n\delta}{\omega_r} \right)^2 \phi'(n) \quad (23)$$

$$\psi(n, j) = (1 - \alpha_o)^2 \left(\frac{n\delta}{\omega_r} \right)^2 \left[\begin{aligned} &\psi'(n, j) \\ &+ (1 - \alpha_o) \frac{2j - n}{2n} \phi'(j) \phi'(n - j) \end{aligned} \right] \quad (24)$$

$$\theta(n, j) = (1 - \alpha_o)^2 \left(\frac{n\delta}{\omega_r} \right)^2 \theta'(n, j) \quad (25)$$

$$\phi'(n) = \int_{R_m}^{R_M} \frac{3\eta(R_o) \tau_o \omega_r^4 l_r^4}{\Lambda(n) \omega_r^2 R_o^2} dR_o \quad (26)$$

$$\psi'(n, j) = \int_{R_m}^{R_M} \frac{3\eta(R_o) \tau_o \omega_r^4 l_r^4}{\Lambda(j) \Lambda(n - j) \omega_r^2 R_o^2} \left[\frac{1}{2} - \frac{\beta_1(n, j)}{\Lambda(n)} \right] dR_o \quad (27)$$

$$\theta'(n, j) = \int_{R_m}^{R_M} \frac{3\eta(R_o) \tau_o \omega_r^4 l_r^4}{\Lambda(j) \Lambda(n + j) \omega_r^2 R_o^2} \left[1 - \frac{\beta_2(n, j)}{\Lambda(n)} \right] dR_o \quad (28)$$

and ω_r and l_r are suitable reference frequency and length scales respectively. Equation (22) has the following approximate solution (accurate to the second order, details are given in Kumar (1991))

$$\begin{aligned} \frac{P_n}{\omega_r^2 l_r^2} = & c_n e^{-\lambda_n X/l_r} + \sum_{j=1}^{n-1} \frac{\psi(n, j) c_j c_{n-j}}{(\lambda_j + \lambda_{n-j})^2 - \lambda_n^2} e^{-(\lambda_j + \lambda_{n-j})X/l_r} \\ & + \sum_{j=1}^{N-n} \frac{\theta(n, j) \bar{c}_j c_{n+j}}{(\lambda_j + \lambda_{n+j})^2 - \lambda_n^2} e^{-(\lambda_j + \lambda_{n+j})X/l_r} \end{aligned} \quad (29)$$

Using the solution given by equation (29) and the momentum equation (Kumar(1991)) the following relation for the conditions at the wall may be obtained

$$\begin{aligned} (\alpha_o - 1) \left(\frac{n\delta}{\omega_r} \right)^2 \frac{X_n(0)}{l_r} = & \lambda_n c_n + \sum_{j=1}^{n-1} \frac{(\lambda_j + \lambda_{n-j}) \psi(n, j) c_j c_{n-j}}{(\lambda_j + \lambda_{n-j})^2 - \lambda_n^2} \\ & + \sum_{j=1}^{N-n} \frac{(\lambda_j + \lambda_{n+j}) \theta(n, j) \bar{c}_j c_{n+j}}{(\lambda_j + \lambda_{n+j})^2 - \lambda_n^2} \end{aligned} \quad (30)$$

In the case of identical bubbles, we have

$$\eta(R_o) = \eta' \delta (R_o - R'_o) \quad (31)$$

where η' is the total number of bubbles per unit liquid volume and R'_o is the radius of the bubbles. It can be seen that above result reduces to the result for identical bubbles given in Kumar (1991).

For purpose of illustration we examine a bubble layer containing bubbles of radii between 10.0 μm and 100.0 μm under the water tunnel conditions.

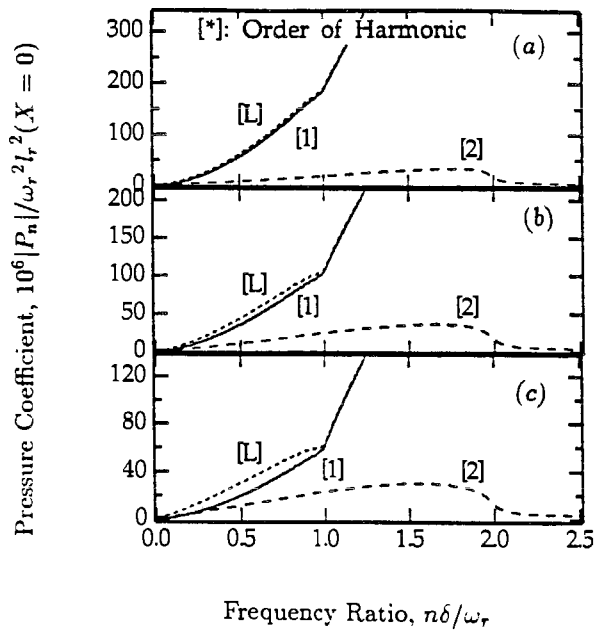


Figure 4. The frequency response of a bubbly layer with a given size distribution of bubbles; $|P_n|/\omega_r^2 l_r^2(X=0)$ is plotted against the frequency ratio, $n\delta/\omega_r$, for the first two harmonics and the linear solution for (a) $m=2$, (b) $m=3$ and (c) $m=4$. The parameters: $X_n(0)/l_r=0.0002$, $\alpha_0=0.05$ and the ambient conditions are for the water tunnel.

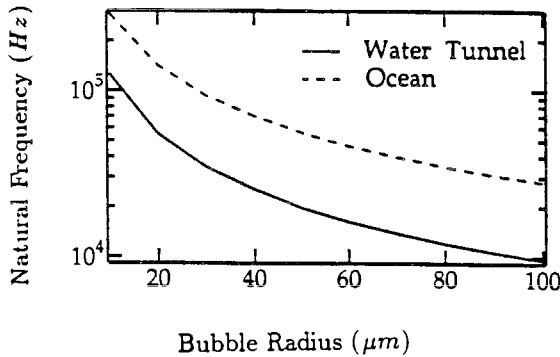


Figure 5. Natural frequency of a single bubble for water tunnel and ocean conditions.

The largest natural frequency of the bubble and the largest bubble radius present in cloud are convenient choices for the reference frequency, ω_r and the reference length scale, l_r respectively. In the sample calculations the coefficients, $c'(n)$, $\psi'(n, j)$ and $\theta'(n, j)$ were evaluated using equations (26), (27) and (28) respectively. The integrals were evaluated numerically using the trapezoidal rule and Richardson extrapolation was used to estimate the value of the integral for zero step size. The parameters Λ_n , $\beta_1(n, j)$ and $\beta_2(n, j)$ were calculated from equations (7), (8) and (9), and λ_n , $\psi(n, j)$ and $\theta(n, j)$ could then be calculated using equations (23)–(25). Equation (30) was then solved using a Newton-Raphson scheme to calculate the constants c_n for a given amplitude of wall oscillation, $X_n(0)/l_r$. Knowing c_n , the amplitude of

pressure oscillation could be calculated from the equation (29). Using this solution, the values of R_n/R_0 were calculated for different values of R_0 and the amplitude of R_n/R_0 is checked to insure that it is less than unity. Note that, equation (30) is similar in structure to the equation (5) and hence the solution is nonzero only at harmonics of the excitation frequency. Once again calculations of up to 20 harmonics were found to be sufficient.

Numerical results were computed for a number of typical cases. For each case the results were obtained for the size distribution density parameter, $m=2, 3, 4$ (see equation (1)) and the value of N^* was adjusted to obtain the required value of the void fraction. The results for six different cases were obtained in order to investigate the effect of changes in void fraction, ambient conditions and amplitude of wall oscillation.

A typical frequency response of the cloud is shown in Fig. 4 for the water tunnel conditions. This illustrates the features of the frequency response common to all cases. The amplitude of pressure oscillation for the fundamental and the second harmonic, which are marked [1] and [2] respectively, as well as the solution obtained from the linearized analysis which is marked [L], are shown. Amplitudes of higher harmonics were found to be negligible. The frequency ratio is the ratio of the actual frequency at which the response occurs to the reference frequency and thus the abscissa represents ω_f/ω_r for the line marked [1] and [L] and $2\omega_f/\omega_r$ for the line marked [2]. It is seen that the amplitude of first harmonic pressure oscillation increases with increasing excitation frequency. The reason for this is that there is a larger number of smaller bubbles, for which the natural frequency of the bubble is larger. Thus for larger frequency ratios (excitation frequencies) a larger number of bubbles are excited at their natural frequency thus leading to an increase in the amplitude of the pressure oscillation. The *stiff* behaviour of bubbles whose natural frequencies are less than the excitation frequency (seen in Kumar (1991) as a response to the *super-resonant* excitation ($\omega_f > \omega_b$), applied to the cloud of identical bubbles) also contributes to an increase in the amplitude of pressure oscillation.

Fig. 5 shows the natural frequency of the bubble for the water tunnel and the ocean conditions. It is clear that smaller bubbles have larger natural frequencies. When the wall is oscillated at a frequency, ω_f , the bubbles with their natural frequency equal to ω_f are excited with the largest amplitude. Because of the nonlinearity present in the system, the flow variables oscillate at the harmonics of the excitation frequency, ω_f . Thus, the pressure oscillation at $2\omega_f$ excites bubbles with their natural frequency equal to $2\omega_f$ and since, the number of bubbles with the natural frequency, $2\omega_f$, is larger than the number of bubbles with the natural frequency, ω_f , the response resulting from the bubbles with natural frequency of $2\omega_f$ may be significant and may be larger for larger values of m . In other words, the excitation may cascade towards higher frequencies. We shall refer to this mechanism as *harmonic cascading*.

The ratio of amplitude of the second harmonic to the amplitude of the first harmonic increases for larger values of the parameter, m (Fig. 4). This could be expected from the above description of the mechanism

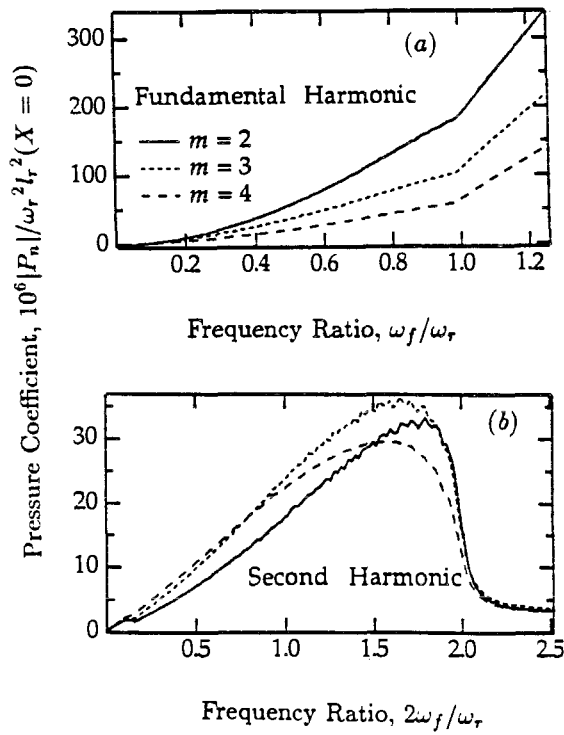


Figure 6. The effect of variation in the bubble size density distribution slope, m , on the (a) first and (b) second harmonic; $|P_n|/\omega_r^2 l_r^2 (X=0)$ is plotted against the frequency ratio, (a) ω_f/ω_r and (b) $2\omega_f/\omega_r$ respectively. The parameters: $X_n(0)/l_r = 0.0002$, $\alpha_o = 0.05$ and the ambient conditions are for the water tunnel.

of *harmonic cascading*. Note that, the linear solution is larger than the first harmonic and the difference between the linear solution and the first harmonic is larger for larger values of m . For excitation frequencies larger than the reference frequency, ω_r , the amplitude of second harmonic is very small and the difference between the linear and nonlinear solutions is also very small. This could be anticipated since ω_r is the highest natural frequency present in the cloud and the effect of *harmonic cascading* is expected to decrease for wall oscillation frequencies larger than $0.5\omega_r$. For excitation frequencies up to $0.5\omega_r$, *harmonic cascading* remains an important effect with the amplitude of second harmonic becoming larger than the amplitude of first harmonic for $m = 4$. For excitation frequencies larger than $0.5\omega_r$, the increase is due to the collective response of the bubbles to the excitation. It is seen that the pressure oscillation decays rapidly away from the wall, decaying to very small values at a distance of $4l_r$ from the wall.

Frequency responses for different values of the size density distribution slope, m , are compared in the Fig. 6. The void fraction is same for all cases. It appears that an increase in the value of m reduces the amplitude of the first harmonic. For a given value of the void fraction, the number of bubbles is larger for larger values of m and the reduction in the amplitude of pressure oscillation may be caused by the increased damping in the system due to the larger number of bubbles. The weaker response for increased void fraction (also seen for a layer of identical bubbles (Kumar

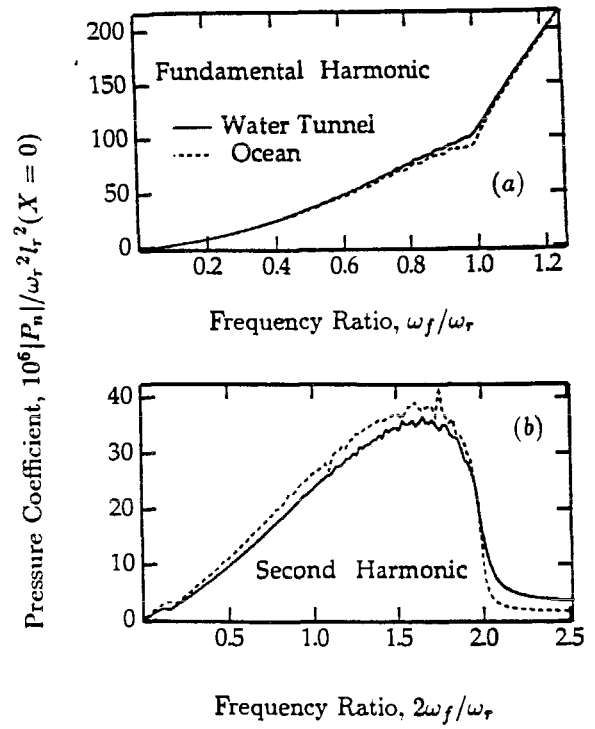


Figure 7. The effect of variation in ambient conditions on the frequency response of the bubbly layer; $|P_n|/\omega_r^2 l_r^2 (X=0)$ for the (a) fundamental and the (b) second harmonic is plotted against the frequency ratio, (a) ω_f/ω_r and (b) $2\omega_f/\omega_r$, respectively for $m = 3$. The parameters: $X_n(0)/l_r = 0.0002$ and $\alpha_o = 0.05$.

(1991)) may also be caused by an increase in the number of bubbles. Note that the amplitude of the second harmonic is not strongly effected by change in the value of m .

The effect of changes in ambient conditions on the frequency response are shown in Figs. 7. Clearly the effect is not a strong one. However, it does appear that the ocean conditions do promote a little stronger *harmonic cascading*. This may be explained as follows. The *super-resonant* ($\omega_f > \omega_b$) excitation of the bubbles which have natural frequencies less than the excitation frequency contributes significantly to the amplitude of the fundamental harmonic and this is not strongly influenced by reduction in the viscous and surface tension parameters for the ocean conditions. However, bubble dynamics play a stronger role in the generation of the second harmonic through *harmonic cascading* and thus increase in the amplitude of the second harmonic (with reduced effect of viscosity and surface tension at the ocean conditions) may be expected. Hence, stronger *harmonic cascading* can be expected for the ocean conditions.

The effect of changes in the void fraction on the layer is shown in Fig. 8. It is clear that higher void fraction reduces the magnitudes of both the first and the second harmonic. As explained earlier, this may be due to larger damping due to increased number of bubbles.

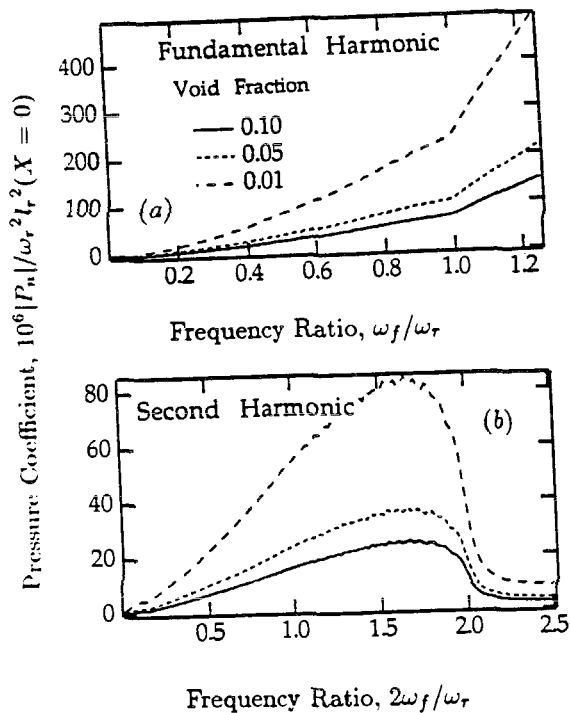


Figure 8. The effect of variation in void fraction on the frequency response of the bubbly layer; $|P_n|/\omega_r^2 l_r^2 (X=0)$ for the (a) fundamental and the (b) second harmonic is plotted against the frequency ratio, (a) ω_f/ω_r and (b) $2\omega_f/\omega_r$, respectively for $m=3$. The parameters: $X_n(0)/l_r=0.0002$ and the ambient conditions are for the water tunnel. Values of void fraction, α_0 , of 0.01, 0.05 and 0.10 are used.

6. LIMITATIONS

In this section we shall examine the various limitations of the present model. The limitation imposed by the continuum mechanics model have been discussed in detail by d'Agostino and Brennen (1988) and so we focus here on additional considerations necessary in the present analysis.

First the amplitude of the radius oscillation is required to be small; in particular, $|R_n/R_0| \ll 1$ must be satisfied. This is also required to avoid the following instability in the bubble dynamics. For pressure oscillations exceeding a threshold value, the bubbles larger than a critical size are known to grow to a large size and then collapse violently (Flynn(1964)). This will not occur if the ratio of the maximum size of the bubble to the equilibrium bubble radius is less than 2.0 (Flynn (1964)). Moreover, the effect of damping is also reduced for large bubbles. These restrictions place an upper limit on the excitation for the present analyses. In practice, $|R_n/R_0| \ll 1$ is expected to dictate the maximum applicable excitation for which the theory remains applicable.

The range of void fraction, for which present theory may be applied, is also bounded by an upper and a lower limit. The lower limit of the void fraction is determined by maximum bubble separation required under continuum assumption as well as requirement of maximum permissible amplitude of radius oscillation, $|R_n/R_0|$. The upper limit on void fraction is

determined by the requirement of local pressure disturbance to be negligible in comparison to the global pressure oscillation (d'Agostino and Brennen (1988)).

The phenomena of rectified diffusion results in slow growth of the equilibrium size of a bubble (Hsieh and Plesset (1961)). Thus, the theory can be applied to the bubbly layers subject to steady state oscillation for long periods only if the equilibrium size, R_0 is tracked and the values appropriate to a particular time are employed.

7. SOME PRACTICAL OBSERVATIONS

Though limited to small amplitude oscillations and thus to a small excitation, the qualitative phenomena uncovered here are valuable to bear in mind when interpreting some of the practical observations of the response of bubbly mixtures. In particular, *harmonic cascading* should be present in many practical situations. Measurements of spectra reported by Mellen (1954) and Blake (1986) appear to contain peaks which may be due to *harmonic cascading*. The results of Arakeri and Shanmuganathan (1985) do not exhibit *harmonic cascading*. However, that may be due to lack of variation in the size of bubbles generated by electrolysis. It may be important to keep this in mind while designing experiments for evaluating interactive effects in bubbly mixtures. It is particularly important to note that most of the spectra reported in the literature have been made using half octave frequency resolution. Clearly, a finer spectra resolution in the spectra measurement is required in order to unambiguously resolve *harmonic cascading*.

8. SUMMARY AND CONCLUSIONS

In this work we have studied the nonlinear effects which can occur when a plane wall bounding a bubbly liquid oscillates in a direction normal to itself.

The phenomena of *harmonic cascading* is seen to take place in a bubbly mixture containing bubbles of different sizes. *Harmonic cascading* occurs when a low frequency excitation applied to the layer at a frequency, ω_f , results in a large amplitude of oscillation at the frequency of $2\omega_f$ due to presence of a large number of bubbles with natural frequency of $2\omega_f$. The ratio of the amplitude of the second harmonic to the amplitude of the first harmonic defines the extent of *harmonic cascading*. This ratio increases with an increase in the number of small bubbles relative to the number of large bubbles. It is noteworthy that the phenomena of *harmonic cascading* can only be modelled by a nonlinear model because the linearized models do not allow for such harmonic generation.

Larger values of the void fraction cause a reduction in the amplitude of pressure oscillation in all cases. This may imply reduced acoustic noise in the bubbly mixtures (observed experimentally by Arakeri and Shanmuganathan (1985)) and damage potential in cavitating flows. Furthermore, the larger number of bubbles present at large void fractions may cause stronger dissipation and a reduced amplitude of oscillation.

9. ACKNOWLEDGEMENTS

The authors are grateful for the support of Office of Naval Research under contract N 000167 - 85 - K - 0165.

REFERENCES

- Arakeri, V.H. and Shanmuganathan, V. 1985. *On the Evidence for the Effect of Bubble Interference on Cavitation Noise*. J. Fluid Mech., Vol. 159, pp. 130-150.
- Biesheuvel A. and van Wijngaarden, L. 1984. *Two Phase Flow Equations for a Dilute Dispersions of Gas Bubbles in Liquid*. J. Fluid Mech., Vol. 148, pp. 41-52.
- Birnir, B. and Smereka, P. 1990. *Existence Theory and Invariant Manifolds of Bubble Clouds*. Comm. on Pure Appl. Math., John Wiley and Sons, New York, Vol. XIII, pp. 363-413.
- Blake, W.K. 1986. *Propeller Cavitation Noise: The Problems of Scaling and Prediction*. Int. Symp. on Cav. and Multiphase Flow Noise, pp. 89-99.
- Blake, W. K., Wolpert, M. J. and Geib, F. E. 1977. *Cavitation Noise and Inception as Influenced by Boundary Layer Development on a Hydrofoil*. J. Fluid Mech., Vol. 80, pp. 617-640.
- Brennen, C. E. and Ceccio, S. L. 1989. *Recent Observations on Cavitation and Cavitation Noise*. Third Int. Symp. on Cavitation Noise and Erosion in Fluid Systems, San Francisco, CA, Dec. 1989, pp. 67-78.
- Ceccio, S. L. and Brennen, C. E. 1991. *The Dynamics and Acoustics of Travelling Bubble Cavitation*. To appear in the J. Fluid Mech.
- Chahine, G.L. 1982. *Pressure Field Generated by the Collective Collapse of Cavitation Bubbles*. IAHR symposium on Operating Problems of Pump Stations and Power Plants, Amsterdam, Netherlands, Vol.1 (2), pp. 1-12.
- d'Agostino, L. and Brennen, C.E. 1988. *Linearized Dynamics of Spherical Bubble Clouds*. J. Fluid Mech., Vol. 199, pp. 155-176.
- Devin C. Jr. 1959. *Survey of Thermal, Radiation and Viscous Damping of Pulsating Air Bubbles in Water*. J. Acous. Soc. Am., Vol. 31 (12), pp 1654-1667.
- Eller, A. and Flynn, H.G. 1969. *Generation of Subharmonics of Order One-Half by Bubbles in Sound Field*. J. Acous. Soc. Am., Vol. 46, No.3 (2), pp. 722-727.
- Flynn, H.G. 1964. *Physics of Acoustics Cavitation in Liquids*. Physical Acoustics - Principles and Methods, ed. W. P. Mason, Vol. 1, Part. B, Academic Press, pp. 57-172.
- Gates, E.M. and Acosta, A.J. 1978. *Some Effects of Several Free Stream Factors on Cavitation Inception on Azisymmetric Bodies*. 12th Symp. on Naval Hydrodynamics, Washington, D.C.
- Kumar, S. 1991. *Some Theoretical and Experimental Studies of Cavitation Noise*. Ph. D. Thesis, Div. of Engg. and Appl. Sci., Calif. Inst. of Tech., Pasadena, CA 91125.
- Lauterborn, W. 1976. *Numerical Investigation of Nonlinear Oscillations of Gas Bubbles in Liquids*. J. Acous. Soc. Am., Vol. 59(2), pp. 283-293.
- Maeda, M., Yamaguchi, H. and Kato, H. 1991. *Laser Holography Measurement of Bubble Population in Cavitation Cloud on a Foil Section*. 1st ASME/JSME Conf., Portland, Oregon, June 1991, FED Vol. 116, pp. 67-75.
- Marboe, M. L., Billet, M. L. and Thompson, D. E. 1986. *Some Aspects of Travelling Bubble Cavitation and Noise*. Int. Symp. on Cavitation and Multiphase Flow Noise, ASME, FED Vol. 45, pp. 119-126.
- Mellen, R.H. 1954. *Ultrasonic Spectrum of Cavitation Noise in Water*. J. Acous. Soc. Am., Vol. 26 (3), pp. 356-360.
- Omta, R. 1987. *Oscillations of a Cloud of Bubbles of Small and Not So Small Amplitude*. J. Acous. Soc. of Am., Vol. 82, pp. 1018-1033.
- Plesset, M.S. 1949. *The Dynamics of Cavitation Bubbles*. Trans. ASME, J. Appl. Mech., Sept. 1949, pp. 277-282.
- Plesset, M.S. and Hsieh, D.Y. 1960. *Theory of Gas Bubble Dynamics in Oscillating Pressure Fields*. Phys. of Fluids, Vol. 3(6), pp. 882-892.
- Plesset, M.S. and Prosperetti, A. 1977. *Bubble Dynamics and Cavitation*. Ann. Rev. Fluid Mech., Vol. 9, pp. 145-185
- Prosperetti, A. 1975. *Nonlinear Oscillations of Gas Bubbles in Liquids: Transient Solutions and the Connection Between Subharmonic Signal and Cavitation*. J. Acous. Soc. Am., Vol. 57(4), pp. 810-821.
- Prosperetti, A. 1977. *Application on Subharmonic Threshold to the Measurement of the Damping of Oscillating Gas Bubbles in Liquids*. J. Acous. Soc. Am., Vol. 61 (1), pp. 17-27.
- Tangren R.F., Dodge C.H. and Seifert H.S. 1949. *Compressibility Effects in Two-Phase Flows*. J. Appl. Phys., Vol.20, pp. 637-645.
- van Wijngaarden, L. 1964. *On the Collective Collapse of Large Number of Gas Bubbles in Water*. Proc. of 11th Int. Cong. of Appl. Mech., Springer-Verlag, Berlin, pp. 854-861.